A mathematical model of the hypothalamic network controlling the pulsatile secretion of reproductive hormones

Margaritis Voliotis[1,2,*], Xiao Feng Li[3], Kevin T. O'Byrne[3], Krasimira Tsaneva-Atanasova[1,2,*],

1 Department of Mathematics and Living Systems Institute, College of Engineering, Mathematics and Physical Sciences, University of Exeter, Exeter, EX4 4QF, UK

2 EPSRC Centre for Predictive Modelling in Healthcare, University of Exeter, Exeter, EX4 4QJ, UK.

3 Department of Women and Children's Health, School of Life Course Sciences, King's College London, London SE1 1UL, UK.

* M.Voliotis@exeter.ac.uk, K.Tsaneva-Atanasova@exeter.ac.uk

Abstract

Reproduction critically depends on the pulsatile secretion of gonadotrophin-releasing hormone (GnRH) from the hypothalamus. This ultradian rhythm drives the secretion of gonadotrophic hormones (LH and FSH) from the pituitary gland, which are critical for gametogenesis and ovulation, and its frequency is regulated throughout the life course to maintain normal reproductive health. However, the precise mechanisms controlling the pulsatile GnRH dynamics are unknown. Here, we propose and study a novel mathematical model of a population of neurones in the arcuate nucleus (ARC) of the hypothalamus that co-expresses three key modulators of GnRH secretion: kisspeptin; neurokinin B (NKB); and dynorphin (Dyn). The model highlights that positive feedback in the population exerted by NKB and negative feedback mediated by Dyn are the two key components of the pulse generator, which operates as a relaxation oscillator. Furthermore, we use the model to study how external inputs modulate the frequency of

the pulse generator, a prediction that can be readily tested in-vivo using optogenetically-driven stimulation. Finally, our model predicts the response of the system to various neuropharmacological perturbations and reconciles inconsistent experimental observations following such interventions in-vivo. We anticipate that our model in combination with cutting-edge, in-vivo techniques, allowing for neuronal stimulation and recording, will set the stage for a quantitative, system-level understanding of the GnRH pulse generator.

Introduction

Reproduction is fundamental for the survival of species and is therefore tightly regulated even in the simplest of living organisms. In mammals, reproduction is controlled by the coordinated action of the brain, the pituitary gland, and the gonads. Within the brain a neuronal clock drives the periodic release of gonadotrophin-releasing hormone (GnRH). The operation of this GnRH pulse generator at a frequency appropriate for the species is critical for the generation of gonadotrophin hormone signals (luteinizing hormone, LH; and follicle-stimulating hormone, FSH) by the pituitary glad, which stimulate the gonads and set in motion gametogenesis and ovulation. However, the mechanisms underlying the GnRH pulse generator remain poorly understood.

GnRH is produced from specialised neurones, known as GnRH neurones, and its secretion into the pituitary is controlled by upstream hypothalamic signals [1]. Neuropeptide kisspeptin has been identified as a key regulator of GnRH as both humans and rodents with inactivating mutations in kisspeptin or its receptor fail to progress through puberty or show normal pulsatile LH secretion [2–4]. Within the hypothalamus, two major kisspeptin producing neuronal populations are located in the arcuate nucleus (ARC) and in the preoptical area [5] or the anteroventral periventricular (AVPV)/rostral periventricular (PeN) continuum in rodents [6]. Moreover, the invariable association between neuronal activity in the ARC and LH pulses across a range of species from rodents to primates [7] has been suggestive that the ARC is the location of the GnRH pulse generator, and therefore the ARC kisspeptin neurones, also known as KNDy for co-expressing neurokinin B (NKB) and dynorphin (Dyn) alongside kisspeptin [8], constitute the core of the GnRH pulse generator.

Although animal studies have shown that the KNDy population plays a critical role in the regulation of GnRH, there has been relatively little information on the regulatory mechanisms involved in generating and sustaining pulsatile dynamics. Pharmacological modulators of kisspeptin, NKB and Dyn signalling have been extensively used to perturb the system and study the effect on the activity of the neuronal population (using hypothalamic multiunit activity (MUA) volleys as a proxy), as well as on downstream GnRH/LH dynamics [9–12]. For example, it has been shown that kisspeptin (Kp-10) administration does not affect MUA volleys in the ovariectomised rat [9], suggesting that kisspeptin is relaying the pulsatile signal to GnRH neurones rather than generating it. On the contrary, administration of NKB or Dyn modulates MUA volley frequency in the ovariectomised goat [11], suggesting a more active role for these neuropeptides in the generation of the pulses. Deciphering, however, the role of NKB has been problematic, and there exist conflicting data showing either an increase or decrease of LH levels in response to administration of a selective NKB receptor agonist (senktide) [10, 12, 13]. Recently, a study combining optogenetics, with whole-cell electrophysiology and molecular pharmacology has shed light on the action of neuropeptides NKB and Dyn and their role in controlling reproductive function [14]. The key mechanistic insight from this study was that NKB functions as an excitatory signal by depolarising cells at the post-synaptic end, while Dyn functions as an inhibitory signal by suppressing the action of NKB at the presynaptic end.

Here, motivated by these experimental findings, we develop a mathematical model of the ARC KNDy population. The model is based on a network description of the population and captures two important processes: secretion of Dyn and NKB by individual neurones; and regulation of the population firing activity by the two neuropeptides. The model predicts that the KNDy population can indeed generate and sustain oscillatory firing dynamics similar to the multi-unit activity (MUA) volleys observed in-vivo [12] and provides insight on mechanism underlying pulse generation. Furthermore, our model predicts the response of the system to various neuropharmacological perturbations and reconciles inconsistent experimental observations following such interventions in-vivo. Finally, we perform global sensitivity analysis to uncover possible pathways through which the dynamics of the system can be modulated. Our model complements existing phenomenological models of GnRH dynamics [15], and makes testable in-vivo predictions

that will shed light on the mechanisms underlying GnRH regulation.

Results

A mathematical network model describing the ARC KNDy population

We use a mathematical network model (Fig 1A) to describe and study the collective dynamics of KNDy neurones in the ARC. The model describes the dynamics of M synaptically connected KNDy neurones using a set of coupled ordinary differential equations (ODEs). For each neurone i, we use variables D_i and N_i, to denote the concentration of Dyn and NKB, secreted at its synaptic ends; and variable v_i to denote its firing rate, measured in spikes/min. The ODEs describing the dynamics of neurone i in the population are:

$$\frac{dD_i}{dt} = f_D(v_i) - d_D D_i; \tag{1}$$

$$\frac{dN_i}{dt} = f_N(v_i, D_i) - d_N N_i; \tag{2}$$

$$\frac{dv_i}{dt} = f_v\left(\{v_j, N_j\}_{j\in\text{neigh}(i)}\right) - d_v v_i. \tag{3}$$

Parameters d_D, d_N and d_v prescribe the characteristic timescale for each variable. In particular, parameters d_D and d_N correspond to the rate at which Dyn and NKB are lost (e.g., due to diffusion or active degradation), while d_v relates to the rate at which neuronal activity resets to its basal level. Functions f_D, f_N give the secretion rate of Dyn and NKB, respectively, while function f_v encodes how the firing rates changes in response to synaptic inputs. Crucially, the activity of neurone i, v_i, depends on the firing rate and secreted level of NKB of all other neurones j that are synaptically connected to it. This dependence is denoted by the curly brackets notation in the arguments list of f_v. Synaptic connections are summarised by the adjacency matrix, A: a binary, square $(M \times M)$ matrix with $A_{ij} = 1(0)$ indicating synaptic connectivity from neurone i to neurone j. In the model, synaptic connections are formed randomly between all neurones with a constant probability, i.e., $\text{Prob}(A_{ij} = 1) = \bar{c}$.

We use the following sigmoidal (Hill-type) functions to describe regulatory relation-

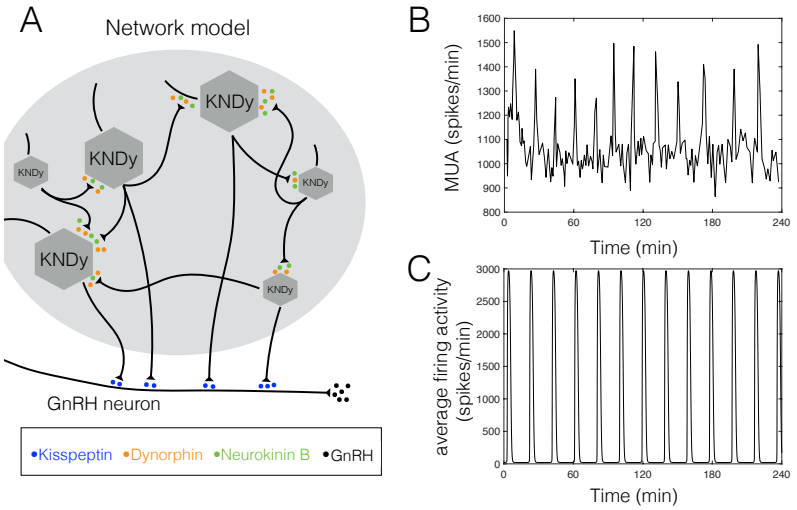

Fig 1. A network model of KNDy neurones in the arcuate nucleus (ARC). (A) Schematic illustration of the dynamical, network model comprising a population of synaptically connected KNDy neurones. In the model, the neuronal firing rate drives the secretion of regulatory neuropeptides dynorphin (Dyn) and neurokinin B (NKB). Furthermore, NKB excites postsynaptic neurones while Dyn inhibits NKB secretion presynaptically. (B) Multi-unit activity (MUA) volleys recorded from the hypothalamus of an ovariectomized rat (data from [12]). (C) The model produces sustained oscillations with explosive spikes of neuronal activity similar to those observed in-vivo. Model parameters were inferred from the data in (B) using an Approximate Bayesian Computation method based on sequential Monte Carlo (ABC SMC; see Material and Methods section) and are listed in Tbl 1.

ships between the variables. In particular, we set the the secretion rate of Dyn and NKB to be:

$$f_D(v) = k_D \frac{v^{n_1}}{v^{n_1} + K_{v,1}^{n_1}};$$
$$f_N(v, D) = k_N \frac{v^{n_2}}{v^{n_2} + K_{v,2}^{n_2}} \frac{K_D^{n_3}}{D^{n_3} + K_D^{n_3}}.$$

That is, neuronal activity stimulates secretion of both neuropeptides, and Dyn represses NKB secretion, which is in agreement with experimental evidence of Dyn inhibiting the action of NKB presynaptically [14]. Neuropeptides secretion is limited by the available neuropeptide pools as well as by other biochemical species driving or regulating the process, therefore in the model we allow saturation of the secretion rate above certain thresholds of v and D, which are set by parameters $K_{v,1}$, $K_{v,2}$ and K_D. Furthermore,

we set

$$f_v\left(\{v_j, N_j\}_{j\in \mathrm{neigh}(i)}\right) = v_0\left(\frac{2}{\exp(-I)+1} - 1\right); I = I_0 + \sum_{j\in neigh(i)} p_v \frac{N_j^{n_4}}{N_j^{n_4} + K_N^{n_4}} v_j,$$

where v_0 is the maximum rate at which the firing rate increases in response to synaptic inputs. The stimulatory effect of NKB (secreted at the presynaptic end) is mediated via G protein-coupled receptor Tacr3 and is manifested as a short-term depolarisation of the postsynaptic neurone [14]. In our equation above, we accommodate this effect by letting the synaptic strength be a function of the secreted NKB. Moreover, parameter p_v sets the maximum strength of the synapse, while parameter K_N sets the level of NKB at which its effect is half-maximal. Finally, parameter I_0 captures synaptic inputs stemming from other neuronal populations or from synaptic noise.

We infer model parameters using the frequency and duty-cycle of the multi-unit activity (MUA) volleys recorded from thehypothalamus an ovariectomized rat [12] (see Material and Methods section). As illustrated in Fig 1B&C, the model can replicate pulses of synchronised activity similar to the MUA signal recorded in-vivo. This finding further supports the hypothesis that KNDy neurones in the ARC constitute the core of the GnRH pulse generator. Furthermore, the model will allow us to study the mechanisms generating and sustaining the rhythmic activation of the KNDy neural network, facilitating our understanding of the relationships underpinning this complex biological system.

A relaxation oscillator drives the pulsatile activity of the KNDy neuronal population

Having shown that the model can reproduce sustained pulses of neuronal activity (see Fig 1B), we move to study the mechanisms driving the phenomenon. To do so, we simplify the network model, and derive a coarse-grained (mean-field) model of the neuronal population comprising three dynamical variables: $\bar{D}$, representing the average concentration of Dyn secreted; $\bar{N}$, representing the concentration of NKB secreted; and $\bar{v}$, representing the average firing activity of the neuronal population. Derivation of the coarse-grained model proceeds by averaging Eq 3 over all neurones (index i); and

expanding (keeping up to leading term) all non-linear functions of D_i, N_i and v_i around the population-averaged values, $\bar{D} = \sum_i D_i/M$,$\bar{N} = \sum_i N_i/M$ and $\bar{v} = \sum_i v_i/M$ (see S1 text). The resulting equations, describing the time evolution of the population-averaged variables, are:

$$\frac{d\bar{D}}{dt} = f_D(\bar{v}) - d_D\bar{D}; \tag{4}$$

$$\frac{d\bar{N}}{dt} = f_N(\bar{v}, \bar{D}) - d_N\bar{N}; \tag{5}$$

$$\frac{d\bar{v}}{dt} = f_v(\bar{v}, \bar{N}) - d_v\bar{v}. \tag{6}$$

All parameters and functions are defined as before (see section above), except for synaptic input I that now takes the form: $I = I_0 + p_v\bar{c}M\frac{\bar{N}^{n_4}}{\bar{N}^{n_4} + K_N^{n_4}}\bar{v}$, where $\bar{c}$ is the average number of synapses that a neurone receives as a fraction of the population size.

To explore the mechanisms underpinning the oscillatory behaviour, we remove Dyn-mediated negative feedback from the system and study the the dynamics of the $(\bar{N}, \bar{v})$ subsystem treating variable $\bar{D}$ as a bifurcation parameter. The result of this analysis is illustrated in Fig 2B and shows that for intermediate values of Dyn the $(\bar{N}, \bar{v})$ exhibits two stable steady states corresponding to the high and low branches shown in Fig 2B. This bistable behaviour, stemming from the non-linear, positive feedback between neuronal activity and NKB secretion, leads to sustained oscillations of neuronal activity when combined with slow negative feedback mediated through Dyn. Furthermore, we expect exogenous inhibitory/excitatory sources, such as distinct neuronal populations or synaptic noise, to be direct modulators of the oscillatory behaviour by altering the dynamic behaviour of the $(\bar{N}, \bar{v})$ sub-system. Indeed, treating the basal synaptic inputs parameter, I_0, as a bifurcation parameter, we find that oscillatory behaviour of the system is limited to a critical range. In particular, as inputs are increased from zero, high-amplitude, low-frequency pulses emerge after a homoclinic bifurcation (Fig 2C; HC point). The value of I_0 at which the bifurcation occurs is equivalent to driving the neuronal population at a rate of approximately 0.024 Hz in the absence of NKB and Dyn modulation. As external excitation ramps up, the frequency of pulses continues to increase, until oscillations disappear altogether through a Hopf bifurcation (Fig 2C; HB point) and the system re-enters a mono-stable regime. In engineering terms, the system

behaves as a relaxation oscillator, where the bi-stable subsystem is successively triggered by external excitation and silenced due to negative feedback. We should note that a sufficiently slow negative feedback can sustain oscillations in the absence of bistabity, however, the combination of bistability with negative feedback is a recurring motif in many biological oscillators [16, 17].

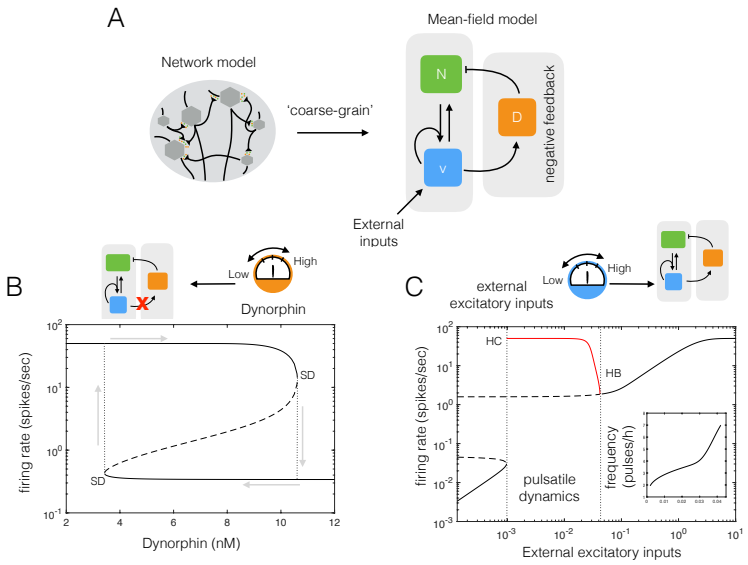

Fig 2. A coarse-grained model gives mechanistic insight into the pulsatile behaviour of the neuronal population. (A) We simplify the network model by deriving a mean-field model of the neuronal population comprising three dynamical variables: $\bar{D}$, representing the average concentration of Dyn secreted; $\bar{N}$, representing the concentration of NKB secreted; and $\bar{v}$, representing the average firing activity of the neuronal population. (B) After disrupting the negative feedback loop (i.e., setting Dynorphin under external control) the system exhibits, for intermediate values of Dynorphin, two stable steady-states (upper and lower solid lines) and an unstable one (dashed line). At the edges of the bistable regime equilibria are lost through a saddle-node bifurcation (SD points). The bistability gives rise to hysteresis as the value of Dyn is varied externally (grey arrows). (C) The coarse-grained model predicts how external excitatory inputs affect the system's dynamics and pulse frequency. As external excitation is increased from zero, high-amplitude, low-frequency pulses emerge after some critical value (HC point; homoclinic bifurcation). The frequency of pulses continues to increase with external excitation until oscillations disappear altogether (HB point; Hopf bifurcation) and the system enters a mono-stable regime. Model parameter values are given in Tbl 1.

The model predicts the response of the system to various neuropharmacological perturbations and reconciles inconsistent experimental observations following such interventions in-vivo

Neuropharmacology is a powerful tool used to study the role of neurotransmitter and neuropeptide signalling on the pulsatile GnRH dynamics. In-vivo, localised administration of drugs that selectively activate or inhibit certain pathways of interest, can shed light on the regulatory mechanism underlying pulse generation and frequency modulation. However, the effect of such neuropharmacological perturbations can appear confusing and difficult to interpret when feedback interactions and non-linearities are present in the system. One notable example, regards senktide (a selective NKB receptor agonist) that appears to be suppressing pulsatile GnRH/LH dynamics in some cases [12,13] while stimulating LH secretion in others [10]. To study this controversial finding, we extend our coarse-grained model to accommodate the effect of two drugs often used to perturb the system in-vivo: senktide, a selective NKB receptor agonist; and nor-BNI, a selective κ-opioid receptor antagonist. We use E to denote the drug concentration injected into the system. As senktide has the same effect as NKB but functions independently, we incorporate it in our model by modifying the expression for the synaptic input I as follows:

$$I = I_0 + p_v \bar{c} M \frac{\bar{N}^{n_4} + E^{n_4}}{\bar{N}^{n_4} + E^{n_4} + K_N^{n_4}} \bar{v}$$

On the other hand, nor-BNI blocks Dyn signalling, therefore we modify function f_N to read:

$$f_N(v, D) = k_N \frac{v^{n_2}}{v^{n_2} + K_{v,2}^{n_2}} \frac{K_D^{n_3} + E^{n_3}}{D^{n_3} + E^{n_3} + K_D^{n_3}}.$$

That is, the antagonist is effectively increasing parameter $K_{v,2}$ in the model.

Figure 3A&B illustrates that the effect of perturbing the system with senktide varies depending on the underlying NKB and Dyn secretion capacity (parameters k_N and k_D in the model). In particular, Fig 3A shows the region over the parameter space (grey area) for which the unperturbed system demonstrates pulsatile dynamics. This region is deformed after senktide administration, and given the system starts from within the oscillatory regime three distinct response types are observed (see Fig 3B; indicative examples are marked with numbers). First, administration of senktide can set the system

in a steady-state of elevated activity after a transient spike (see trace marked 1). Such an effect is consistent with data from diestrus rats, showing that intracerebroventricular administration of senktide to gonadal intact rats in the diestrous phase of the estrous cycle stimulated transiently LH secretion [12]. Second, administration of senktide can increase the pulse frequency (see trace marked 2 and Fig C in S1 text). This type of response is consistent with data showing that intracerebroventricular administration of NKB increases the frequency of multiunit electrical activity (MUA) volleys recorded from the medial basal hypothalamus in the OVX goat [11]. An increase in the frequency of MUA volleys in response to central nor-BNI administration [11] is also in agreement with the model (see Fig B in S1 text). Finally, administration of senktide can suppress pulsatile dynamics setting the system in a low activity steady-state (see trace marked 3). This apparent inhibition of the system through an excitatory agent although counter intuitive is in agreement with the inhibition of hypothalamic MUA volleys and serum LH observed in adult OVX rats after intracerebroventricular administration of senktide [12]. Fig 3C illustrates the effect of perturbing the system with a combination of NKB and nor-BNI. Note, that the combined administration of the two drugs can preserve pulsatile dynamics in cases where senktide alone was suppressing it (see trace 3); in agreement with experimental data showing that nor-BNI blocks the senktide-induced suppression of pulsatile LH secretion in OVX rats [12].

Global sensitivity analysis predicts robustness of oscillatory behaviour to parameter perturbation

The dynamics of GnRH secretion are tightly controlled throughout life, from the initial stages of postnatal development and throughout adulthood [1]. However, the specific pathways through which control is achieved remain mostly unknown. Here, we use the model and global sensitivity analysis to study how various factors could affect the dynamic behaviour of the KNDy population in the arcuate nucleus and hence GnRH secretion. We restrict our focus to three model parameters: the maximum Dyn secretion rate, k_D; the maximum NKB secretion rate k_N; and the magnitude of basal synaptic inputs, I_0. Variability in k_D and k_N capture, for example, regulation of Dyn and NKB levels by sex steroids during menstrual/oestrous cycle [18], whereas changes in

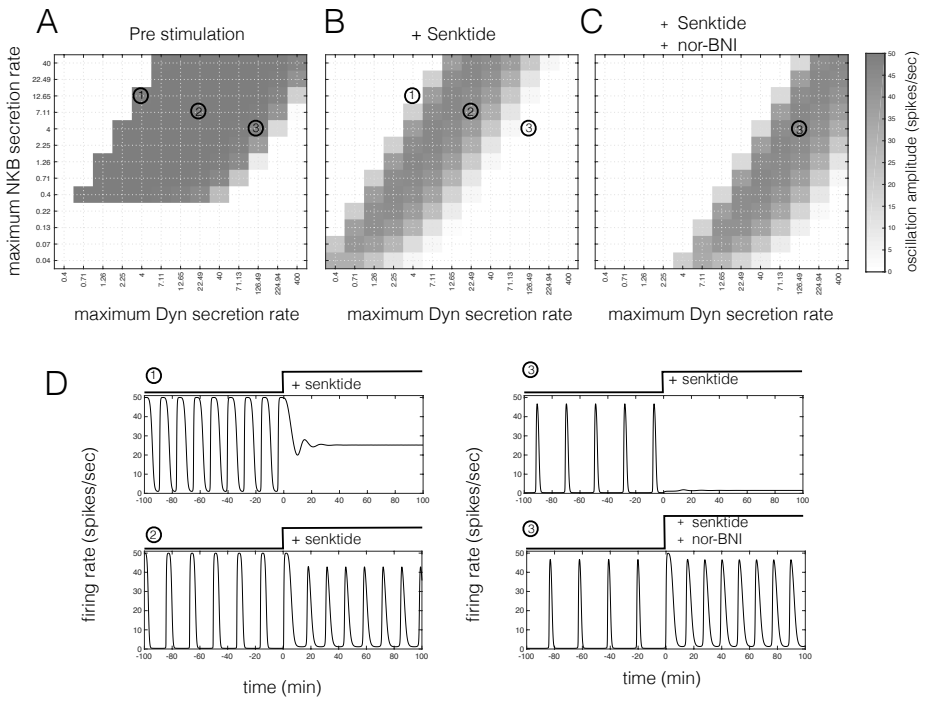

Fig 3. The effect of neuropharmacological perturbations on the activity of the KNDy population. Perturbation of the system with two drugs: senktide, a selective NKB receptor agonist; and nor-BNI, a selective Dyn receptor antagonist. The effect of the perturbation on the dynamics depends on the NKB and Dyn secretion rate. (A) The magnitude of oscillations (grey scale) in the unperturbed system for different levels of maximum NKB and Dyn secretion rate (parameters k_N and k_D in the model). (B) The magnitude of oscillations after perturbing the system with senktide ($E_{senktide} = 60$ pM). (C) The magnitude of oscillations after perturbing the system with senktide ($E_{senktide} = 60$ pM) and nor-BNI ($E_{nor-BNI} = 4.1$ nM) simultaneously. (D) Time-traces of the system activity in response to neuropharmacological perturbations with senktide and nor-BNI. Time-traces correspond to the (k_N, k_D) combinations marked in (A)-(C).

I_0 could map to changes in the excitatory/inhibitory inputs the population receives in developmental stages [1]. To understand how changes in these three parameters affect system dynamics, we vary them independently over a wide range (see Material and Methods section) and study how parameter variability accounts for variance in various critical features of the system's dynamics, e.g., amplitude and period of oscillations.

In Fig 4A, the first order sensitivity indices indicate the proportion of variance of a response feature that is explained by variation in a parameter, while keeping the remaining parameters fixed. First order sensitivity indices, therefore, quantify the effect that single parameter perturbations have on the dynamics of the system. We find that the amplitude of oscillations is most sensitive to changes in the external synaptic

inputs (I_0), and that the maximum magnitude of the response is sensitive to changes in the maximum Dyn secretion rate (k_D). Also, the period of oscillations appears robust to changes in any of the three parameters in isolation. Fig 4B reports the total order sensitivity indices, that is the proportion of variance in a response feature that is explained by variation in a parameter, while allowing other parameters to vary as well. Therefore, the total order sensitivity index of a parameter is a proxy for the effect this parameters has on the dynamics of the systems when co-varied with other parameters. We find that the amplitude as well as the period of oscillations is far more sensitive to combined changes of the parameters. For example, 28% of the total variance in the amplitude of oscillations is attributable to variation of I_0 alone, whereas this figure jumps to more than 76% when variations in other parameters is taken into consideration. Similarly, approximately 83% of the variance in the period of oscillations is explained when parameters are allowed to covary, compared to no more than 14.5% when single parameter variation is considered.

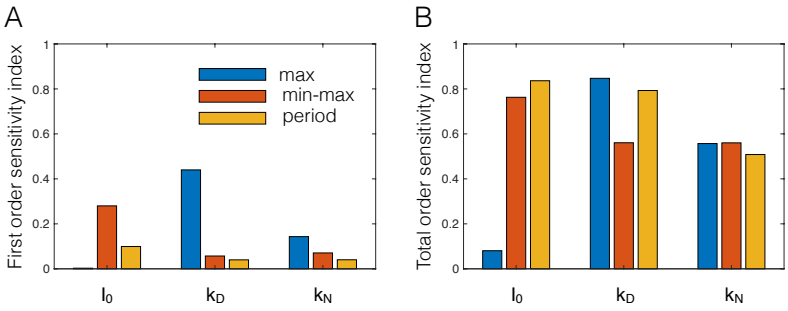

Fig 4. Global sensitivity analysis of the coarse-grained model. Global sensitivity analysis of the coarse-grained model considering maximum response amplitude, minimum response amplitude, amplitude of oscillations, and period of oscillations. First order (A) and total-order (B) sensitivity indices are shown for parameters k_D (maximum rate of Dyn secretion), k_N (maximum rate of NKB secretion) and I_0 (magnitude of external synaptic inputs).

Discussion and Conclusions

Motivated by recent experimental evidence, we developed and studied a mathematical model of the KNDy population in the arcuate nucleus, a population that has been shown to be critical for GnRH pulsatile dynamics [19]. Our model demonstrates that the KNDy population can indeed produce and sustain pulses of neuronal activity that drive

GnRH secretion. The system works as a relaxation oscillator. On the one hand, external excitation and auto-stimulation via NKB signalling effectively allows the population to behave as a bistable switch, firing either at a high or low rate. Moreover, negative feedback through Dyn signalling allows the population to switch between the two activity states in a regular manner, giving rise to pulses of neuronal activity. We found that this mechanism of pulse generation is robust to parameter perturbations. In fact, co-variation of parameters governing, for example, the magnitude of external inputs, and the maximum secretion rates of NKB and Dyn is a more effective way of modulating the systems' oscillatory behaviour (amplitude and frequency). This multi-channel mode of efficient regulation is perhaps not surprising given the system's crucial function, and hints that steroid feedback modulating the dynamics of the pulse generator over the reproductive cycle in female mammals is mediated through multiple, possibly interlinked, pathways.

The proposed model allowed us to study the effect of pharmacological modulators of NKB and Dyn signalling. We find that NKB receptor agonists, such as senktide, could have either an inhibitory or an excitatory effect on the dynamics of the model. We show that this response variability can be explained, for example, by variation in parameters that control the levels of Dyn and NKB secreted by the neurones, which in-vivo are controlled by the sex-steroid milieu. This finding reconciles previous conflicting evidence regarding the effect of senktide on the levels of LH secretion [10, 12, 13]. Our results also highlight the need for a more quantitative understanding of how the sex-steroid milieu affects the NKB and Dyn signalling pathways in the KNDy population. Such an understanding will lead to more accurate interpretation of results from in-vivo neuropharmacological perturbation experiments in various animal models and will shed light on the mechanisms underlying the regulation of GnRH pulsatile secretion.

Furthermore, the model makes a series of testable predictions. First, the model predicts that pulsatile dynamics of the system critically depend on external excitatory or inhibitory signals that the KNDy population receives. For example, low external excitation should silence the system, whereas high excitation should fix the system on a high activity state. This can be tested in-vivo using optogenetics [20–22], that is, by introducing light-sensitive ion-channels into the KNDy neurones and using light to continuously activate or inhibit them, one should be be able to directly control

the generation and frequency of pulses. Moreover, the model predicts that the auto-stimulatory effect of NKB signalling leads to bistable dynamics (see Fig 2B), a property that allows the system to function as a relaxation oscillator [16,17]. Therefore, disrupting the Dyn-mediated negative feedback should leave the system either at a low or high activity state depending on the timing of the disruption relative to the period of the oscillation (see Fig D in S1 text). Testing such predictions will be critical for our understanding of the fundamental dynamic mechanisms governing the GnRH pulse generator behaviour.

Finally, the model can be extended to incorporate the effect of sex hormones, for example, by explicitly modelling circulating concentrations of sex hormones and allowing them to modulate parameters of the current model (e.g., those governing the maximum and minimum secretion rate of NKB and Dyn). This would be a step towards a comprehensive mathematical model that reliably replicates hormonal dynamics in the reproductive axis over longer timescales, spanning, for example, the menstrual/oestrous cycle. We envision that as hormonal measurement techniques advance, enabling accurate, real-time readouts from individuals at low cost, such predictive mathematical models would be a valuable tool to the personalised design of IVF protocols and hormonal contraception methods.

Materials and methods

Bifurcation analysis and numerical experiments

Bifurcation analysis of the coarse-grained model was performed using AUTO-07p [23]. Both the full network model and coarse-grained model were simulated in Matlab using function ode45 (explicit Runge-Kutta (4, 5) solver).

Parameter inference

Parameter inference was performed using an Approximate Bayesian Computation (ABC) method based on sequential Monte Carlo (SMC) [24]. In ABC SMC a population of parameter vectors or particles, θ, is initially sampled form the prior distribution π_0 and propagated with the use of a perturbation kernel through a sequence of distributions

$\pi_i, i = 1, \ldots, \mathcal{T}$. The final distribution $\pi_{\mathcal{T}}(\theta|d(x, x^*) < \epsilon_{\mathcal{T}})$ corresponds to the (approximate) target posterior distribution, where $d(x, x^*)$ is the distance function comparing the simulated dataset x^* to the experimental data x and $\epsilon_{\mathcal{T}}$ is the final error tolerance level. Intermediate distributions are associated with a series of decreasing tolerance levels $\epsilon_i, i = 1, \ldots, \mathcal{T} - 1$, making the transition to $\pi_{\mathcal{T}}$ more gradual and avoiding getting stuck in areas of low probability.

Here, to ensure gradual transition between populations we take $\mathcal{T} = 21$ and set tolerance levels to $\epsilon_i = 10^{(1-0.2i)}, i = 1, \ldots, \mathcal{T}$. The size of each population is set to 500 particles. For each particle, the activity of the KNDy is simulated from $t = 0$ to 6000min, the first 1000 min are discarded, and the remaining time-trace is used to calculate the pulse frequency and duty cycle (defined as the fraction of one period in which KNDy activity is above 50% of the pulse amplitude). The distance function, d, is defined as the sum of the squared relative error in these two summary statistics between the simulated dataset and the data (see Fig 1A; frequency 3.12 pulses/hour; duty cycle 0.15). The prior parameter distributions were chosen as follows: $\log_{10}(d_D) \sim \mathcal{U}(-2, 1)$; $\log_{10}(d_N) \sim \mathcal{U}(-2, 1)$; $\log_{10}(d_v) \sim \mathcal{U}(0, 2)$; $\log_{10}(k_D) \sim \mathcal{U}(-1, 3)$; $k_N \sim \mathcal{N}(40, 4)$ estimate from [25] plus 10% error; $\log_{10}(p_v) \sim \mathcal{U}(-3, 1)$; $K_D \sim \mathcal{N}(0.3, 0.03)$ estimate from [26] plus 10% error; $K_N \sim \mathcal{N}(4, 0.4)$ estimate from [27] plus 10% error; $K_{v,1} \sim \mathcal{U}(1, 3)$; $K_{v,2} \sim \mathcal{U}(1, 3)$; $\log_{10}(I_0) \sim \mathcal{U}(-3, 0)$; where $\mathcal{U}(min, max)$ denotes the uniform distribution in the interval $[min, max]$, and $\mathcal{N}(\mu, \sigma)$ denotes the normal distribution with mean, μ, and standard deviation, σ. For parameters k_N, K_D, K_N, $K_{v,1}$, and $K_{v,2}$ gaussian perturbation kernels were used with standard deviation 4, 0.03, 0.4, 10 and 10 respectively. For all remaining parameter log-normal perturbation kernels were used with standard deviation 0.05. An (approximate) maximum a posteriori (MAP) estimate of model parameters (corresponding to the parameter values of to the most probable particle in the final population) is given in Tbl 1. Histograms of the approximate marginal posterior distribution of each parameter and pairwise scatter plots are shown in Fig A in S1 text.

Global sensitivity analysis

Global sensitivity analysis was performed in Matlab using eFast [28]. For each parameter set, the model was initialised randomly and run from $t = 0$ to 6000 min. Response

Table 1. Model parameters. An (approximate) maximum a posteriori (MAP) estimate of the model parameters obtained using an Approximate Bayesian Computation method based on sequential Monte Carlo (ABC SMC).

No.	Parameter	Description	Value
1	M	Population size	1000 cells
2	d_D	Dyn degradation rate	0.367 min^{-1}
3	d_N	NKB degradation rate	0.351 min^{-1}
4	d_v	firing rate reset rate	4.392 min^{-1}
5	k_D	maximum Dyn secretion rate	218.047 nM min^{-1}
6	k_N	maximum NKB secretion rate	32.33 nM min^{-1}
7	p_v	maximum strength of synaptic inputs	$2.3 \cdot 10^{-3}$ min
8	v_0	maximum rate of neuronal activity increase	13176 spikes min^{-2}
9	K_D	Dyn IC50	0.3 nM
10	K_N	NKB EC50	2.991 nM
11	$K_{v,1}$	firing rate for half-maximal Dyn secretion	810.637 spikes min^{-1}
12	$K_{v,2}$	firing rate for half-maximal NKB secretion	116.09 spikes min^{-1}
13	I_0	basal synaptic inputs	0.0136 (dimensionless)
14	n_1,n_2,n_3, n_4	Hill coefficients	2 (dimensionless)
15	$\bar{c}$	synapse probability	0.5
16	A	adjacency matrix ($M \times M$)	Prob($A_{ij} = 1$) = $\bar{c}$

characteristics, i.e., maximum response amplitude, amplitude of oscillations and the period of oscillation, were calculated from the response trajectory after discarding the first 1000 min.

Table 2. Parameter ranges used in the global sensitivity analysis.

No.	Parameter (units)	max. Value	min Value	Distribution
1	k_D (nM)	400	0.4	$\log_{10}$ uniform
2	k_N (nM)	40	0.04	$\log_{10}$ uniform
3	I_0 (dimensionless)	0.1	0.0001	$\log_{10}$ uniform

Supporting information

S1 text. Supporting Information.

Acknowledgments

KTA and MV gratefully acknowledge the financial support of the EPSRC via grant EP/N014391/1.

References

1. Herbison AE. Control of puberty onset and fertility by gonadotropin-releasing hormone neurons. Nature Reviews Endocrinology. 2016;12(8):452–466. doi:10.1038/nrendo.2016.70.

2. de Roux N, Genin E, Carel JC, Matsuda F, Chaussain JL, Milgrom E. Hypogonadotropic hypogonadism due to loss of function of the KiSS1-derived peptide receptor GPR54. Proceedings of the National Academy of Sciences. 2003;100(19):10972–10976. doi:10.1073/pnas.1834399100.

3. Seminara SB, Messager S, Chatzidaki EE, Thresher RR, Acierno Jr JS, Shagoury JK, et al. The GPR54Gene as a Regulator of Puberty. New England Journal of Medicine. 2003;349(17):1614–1627. doi:10.1056/NEJMoa035322.

4. Kaiser UB. Understanding reproductive endocrine disorders. Nature Reviews Endocrinology. 2015;11(11):640–641. doi:10.1038/nrendo.2015.179.

5. Hrabovszky E. Neuroanatomy of the Human Hypothalamic Kisspeptin System. Neuroendocrinology. 2014;99(1):33–48. doi:10.1159/000356903.

6. Clarkson J, D'Anglemont de Tassigny X, Colledge WH, Caraty A, Herbison AE. Distribution of Kisspeptin Neurones in the Adult Female Mouse Brain. Journal of Neuroendocrinology. 2009;21(8):673–682.

7. Plant TM, Zeleznik AJ. Knobil and Neill's physiology of reproduction. Academic Press; 2014.

8. Lehman MN, Coolen LM, Goodman RL. Minireview: Kisspeptin/Neurokinin B/Dynorphin (KNDy) Cells of the Arcuate Nucleus: A Central Node in the Control of Gonadotropin-Releasing Hormone Secretion. Endocrinology. 2011;doi:10.1210/en.2010-0022.

9. Kinsey-Jones JS, Li XF, Luckman SM, O'Byrne KT. Effects of Kisspeptin-10 on the Electrophysiological Manifestation of Gonadotropin-Releasing Hormone Pulse Generator Activity in the Female Rat. Endocrinology. 2008;149(3):1004–1008. doi:10.1210/en.2007-1505.

10. Navarro VM, Gottsch ML, Chavkin C, Okamura H, Clifton DK, Steiner RA. Regulation of Gonadotropin-Releasing Hormone Secretion by Kisspeptin/Dynorphin/Neurokinin B Neurons in the Arcuate Nucleus of the Mouse. The Journal of Neuroscience. 2009;29(38):11859–11866. doi:10.1523/JNEUROSCI.1569-09.2009.

11. Wakabayashi Y, Nakada T, Murata K, Ohkura S, Mogi K, Navarro VM, et al. Neurokinin B and Dynorphin A in Kisspeptin Neurons of the Arcuate Nucleus Participate in Generation of Periodic Oscillation of Neural Activity Driving Pulsatile Gonadotropin-Releasing Hormone Secretion in the Goat. The Journal of Neuroscience. 2010;30(8):3124–3132. doi:10.1523/JNEUROSCI.5848-09.2010.

12. Kinsey-Jones JS, Grachev P, Li XF, Lin YS, Milligan SR, Lightman SL, et al. The Inhibitory Effects of Neurokinin B on GnRH Pulse Generator Frequency in the Female Rat. Endocrinology. 2011;153(1):307–315. doi:10.1210/en.2011-1641.

13. Sandoval-Guzmán T, E Rance N. Central injection of senktide, an NK3 receptor agonist, or neuropeptide Y inhibits LH secretion and induces different patterns of Fos expression in the rat hypothalamus. Brain research. 2004;1026(2):307–312. doi:10.1016/j.brainres.2004.08.026.

14. Qiu J, Nestor CC, Zhang C, Padilla SL, Palmiter RD, Kelly MJ, et al. High-frequency stimulation-induced peptide release synchronizes arcuate kisspeptin neurons and excites GnRH neurons. eLife. 2016;5:e16246. doi:10.7554/eLife.16246.

15. Clément F, Françoise JP. Mathematical Modeling of the GnRH Pulse and Surge Generator. SIAM Journal on Applied Dynamical Systems. 2007;6(2):441–456. doi:10.1137/060673825.

16. Pomerening JR, Sontag ED, Ferrell JE. Building a cell cycle oscillator: hysteresis and bistability in the activation of Cdc2. Nature Cell Biology. 2003;5(4):346–351. doi:10.1038/ncb954.

17. Goldbeter A. Computational approaches to cellular rhythms. Nature. 2002;420(6912):238–245. doi:10.1038/nature01259.

18. Navarro VM, Castellano JM, McConkey SM, Pineda R, Ruiz-Pino F, Pinilla L, et al. Interactions between kisspeptin and neurokinin B in the control of GnRH secretion in the female rat. American Journal of Physiology - Endocrinology and Metabolism. 2011;300(1):E202–E210.

19. Fergani C, Navarro VM. Expanding the role of tachykinins in the neuroendocrine control of reproduction. Reproduction. 2017;153(1):R1–R14. doi:10.1530/REP-16-0378.

20. Han SY, McLennan T, Czieselsky K, Herbison AE. Selective optogenetic activation of arcuate kisspeptin neurons generates pulsatile luteinizing hormone secretion. Proceedings of the National Academy of Sciences. 2015;112(42):13109–13114. doi:10.1073/pnas.1512243112.

21. Campos P, Herbison AE. Optogenetic activation of GnRH neurons reveals minimal requirements for pulsatile luteinizing hormone secretion. Proceedings of the National Academy of Sciences. 2014;111(51):18387–18392. doi:10.1073/pnas.1415226112.

22. Clarkson J, Han SY, Piet R, McLennan T, Kane GM, Ng J, et al. Definition of the hypothalamic GnRH pulse generator in mice. Proceedings of the National Academy of Sciences. 2017;114(47):E10216–E10223. doi:10.1073/pnas.1713897114.

23. Doedel EJ, Fairgrieve TF, Sandstede B, Champneys AR, Kuznetsov YA, Wang X. AUTO-07P: Continuation and bifurcation software for ordinary differential equations; 2007.

24. Toni T, Welch D, Strelkowa N, Ipsen A, Stumpf MPH. Approximate Bayesian computation scheme for parameter inference and model selection in dynamical systems. Journal of The Royal Society Interface. 2009;6(31):187–202. doi:10.1098/rsif.2008.0172.

25. Ruka KA, Burger LL, Moenter SM. Both Estrogen and Androgen Modify the Response to Activation of Neurokinin-3 and κ-Opioid Receptors in Arcuate Kisspeptin Neurons From Male Mice. Endocrinology. 2015;157(2):752–763. doi:10.1210/en.2015-1688.

26. Yasuda K, Raynor K, Kong H, Breder CD, Takeda J, Reisine T, et al. Cloning and functional comparison of kappa and delta opioid receptors from mouse brain. Proceedings of the National Academy of Sciences. 1993;90(14):6736–6740. doi:10.1073/pnas.90.14.6736.

27. Seabrook GR, Bowery BJ, Hill RG. Pharmacology of tachykinin receptors on neurones in the ventral tegmental area of rat brain slices. European Journal of Pharmacology. 1995;273(1-2):113–119. doi:10.1016/0014-2999(94)00681-V.

28. Marino S, Hogue IB, Ray CJ, Kirschner DE. A methodology for performing global uncertainty and sensitivity analysis in systems biology. Journal of Theoretical Biology. 2008;254(1):178–196. doi:10.1016/j.jtbi.2008.04.011.